Integrated Assessment **2:** 95–110, 2001.

Changes in near-surface temperature and sea level for the Post-SRES CO_2-stabilization scenarios

Michael E. Schlesinger and Sergey Malyshev

Climate Research Group, Department of Atmospheric Sciences, University of Illinois at Urbana-Champaign, 105 S. Gregory Street, Urbana, IL 61801, USA

Received 14 December 2000; revised 12 January 2001

Changes in global near-surface temperature and sea level are calculated from 2000 to 2100 for the Post-SRES (Special Report on Emissions Scenarios) scenarios that stabilize the CO_2 concentration early in the 22nd century. Seven stabilization scenarios are examined together with their corresponding SRES marker scenarios – A1, A1/S450, A1/S550, A1/S650, A2, A2/S550, A2/S750, B1, B1/S450, B2, and B2/S550 – where the number following the S indicates the stabilized CO_2 concentration in parts per million by volume (ppmv). The calculations are performed using an energy-balance-climate/upwelling-diffusion-ocean model for three values of the climate sensitivity, $\Delta T_{2x} = 1.5$, 2.5 and 4.5°C. The resulting reductions in global warming and sea-level rise for the stabilization scenarios relative to their corresponding marker scenario increases with ΔT_{2x} and are greater the lower the stabilized CO_2 concentration. For the S550 stabilization scenarios, the reductions in global warming and sea-level rise in 2100 range from 0.29°C and 3.31 cm for B2/S550 with $\Delta T_{2x} = 1.5$°C, to 1.23°C and 11.81 cm for A2/S550 with $\Delta T_{2x} = 4.5$°C. The percent reductions for the global warming and sea-level rise for each stabilization scenario are almost independent of ΔT_{2x} and range respectively from about 16% and 12% for the A1/S650 scenario to about 39% and 30% for the A1/S450 scenario. The geographical distributions of near-surface temperature change are constructed using a method to superpose the patterns simulated by our atmospheric general-circulation/mixed-layer-ocean model, individually for doubled CO_2 concentration and decupled SO_4 burden. Results are illustrated for the B2 and B2/S550 scenarios for $\Delta T_{2x} = 2.5$°C. The near-surface temperature changes of the B2/S550 scenario in 2100 are everywhere smaller than those for the B2 scenario, with values ranging from about 0.3°C in the tropics to 0.5°C over Antarctica and 0.7°C in the Arctic. The global results of this study are available on the web at: http://crga.atmos.uiuc.edu/research/post-sres.html. We would be pleased to collaborate with other researchers in using these results in impact and integrated-assessment studies.

1. Introduction

In its Special Report on Emissions Scenarios (SRES) [23], the Intergovernmental Panel on Climate Change (IPCC) constructed four families of scenarios for the future emissions of greenhouse gases (GHGs) and anthropogenically emitted sulfur dioxide (SO_2). These scenario families are non-interventionist in that they do not include abatement of GHG emissions for the purpose of climate-change mitigation. For each scenario family there is a "marker" scenario and one or more variants thereof. The SRES marker scenarios differ in their projections of possible future population, gross world productivity (GWP) per person, energy use per unit GWP, and carbon dioxide (CO_2) emission per unit of energy use [37]. Scenario A1 has high economic growth and low population growth; CO_2 emissions are moderate and SO_2 emissions are low. Scenario A2 has low economic growth and high population growth. It results in the highest CO_2 and SO_2 emissions and continued disparity between rich and poor countries. Scenario B1 has moderate economic growth and low population growth, with emphasis on the reduced materialization of the economy and movement away from fossil fuels; CO_2 and SO_2 emissions are low. Scenario B2 has moderate economic growth and moderate population growth, with continued disparity across countries; CO_2 and SO_2 emissions are moderate.

In an earlier study [37], we calculated the time evolution from 2000 to 2100 of the changes in global-mean near-surface temperature and sea level for the four SRES marker scenarios, and we constructed for 2100 the geographical distributions of their near-surface temperature change.

Recently, Post-SRES scenarios have been proposed that modify the SRES marker scenarios such that the CO_2 concentration is stabilized early in the 22nd century. As shown in table 1, there are seven Post-SRES scenarios that stabilize the CO_2 concentration at either 450, 550, 650 or 750 parts per million by volume (ppmv). Stabilization scenarios for these four levels do not exist for all four SRES marker scenarios, and not even a single stabilization level exists for all four markers. The most prevalent stabilization level is 550 ppmv, which exists for all marker scenarios except B1. The reason for this is that the B1 scenario itself leads to a CO_2 concentration of about 550 ppmv by 2100 (see figure 7); including the non-CO_2 greenhouse gases leads to an equivalent CO_2 concentration (the amount of CO_2 required to give the same radiative forcing as all of the greenhouse gases, including CO_2) of over 660 ppmv [3].

In this paper we calculate the time evolution from 2000 to 2100 of the changes in global-mean near-surface temperature and sea level for the seven Post-SRES and four SRES marker scenarios, and we construct geographical distributions of near-surface temperature change for 2100.

In the following we present the emissions for the stabilization and marker scenarios in section 2 and the resulting concentrations in section 3. The calculated radiative forcing and changes in global-mean near-surface temperature and sea level are presented in section 4, and the geographical distributions of near-surface temperature change are presented in section 5. Conclusions are presented in section 6.

Table 1
Scenarios considered in this study.

CO_2 stabilization level (ppmv)	Designator	Model	References[a]
None	A1	Asian-Pacific	Jiang et al. [10,11]
650	A1/S650	Integrated Model	
550	A1/S550	(AIM)	
450	A1/S450		
None	A2	Atmospheric	Sankovski et al. [27,28]
750	A2/S750	Stabilization	
550	A2/S550	Framework (ASF) model	
None	B1	AIM	de Vries et al. [3], de Vries personal communication
450	B1/S450		
None	B2	MESSAGE-MACRO model	Riahi and Roehrl [25,26]
550	B2/S550		

[a] The first reference is for the SRES marker scenario and the second reference is for the Post-SRES stabilization scenario(s).

2. Emissions

The emissions of CO_2, CH_4, N_2O and SO_2 for the 11 scenarios are shown respectively in figures 1–4 and the emissions of CFC-11 and CFC-12 are shown in figure 5. The data shown in figures 1–4 have been provided us by Drs. T. Morita, T. Masui and K. Jiang for the A1-related and B1-related scenarios, A. Sankovski for the A2-related scenarios, and K. Riahi and R.A. Roehrl for the B2-related scenarios. The CFC-11 and CFC-12 emissions are the same as those used by us in our study of the climate changes for SRES marker scenarios [37]. The marker scenarios used here are the final SRES scenarios [23] which differ somewhat from the preliminary SRES marker scenarios used by Schlesinger et al. [37].

The CO_2 emissions extend to 2300 for the A1 stabilization scenarios and were calculated by the AIM Stabilization Scenario Generator (SSG) [17,18]. The emissions scenarios for all species other than CO_2 extend only to 2100. For this reason our climate-change calculations extend only to 2100. However, in section 3 we present the CO_2 concentrations (and emissions) to 2300 for the A1 scenarios to show that the concentrations do indeed stabilize at their targeted values.

It is evident in figures 1–4 that the emissions in 2000 for some of the stabilization scenarios differ from the emissions for their corresponding marker scenario. This reflects the fact that the Post-SRES stabilization scenarios, unlike the SRES marker scenarios [23], have not been standardized

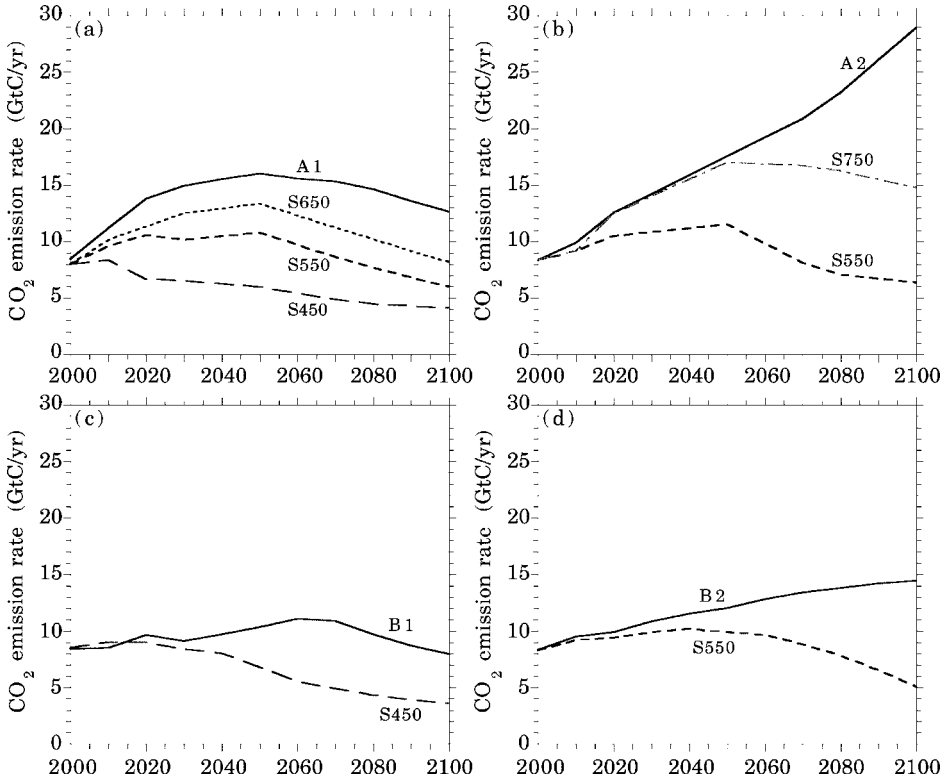

Figure 1. Annual CO_2 emission rate for the A1 (a), A2 (b), B1 (c) and B2 (d) SRES marker scenarios and their corresponding Post-SRES stabilization scenarios.

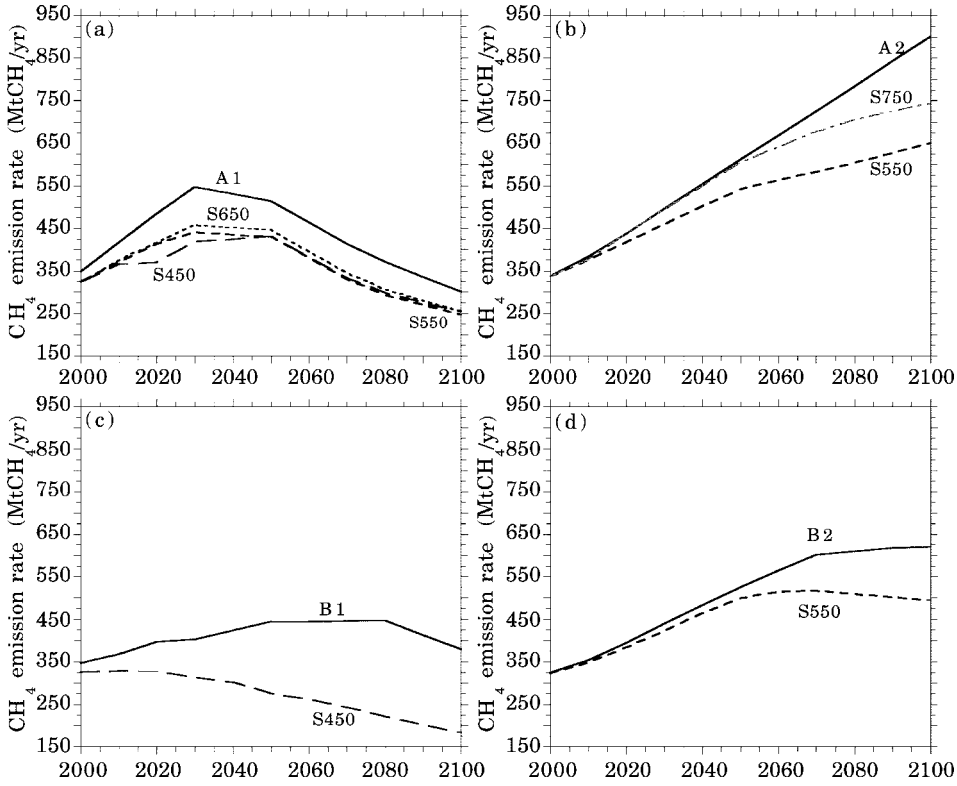

Figure 2. As in figure 1, except for the CH_4 emission rates.

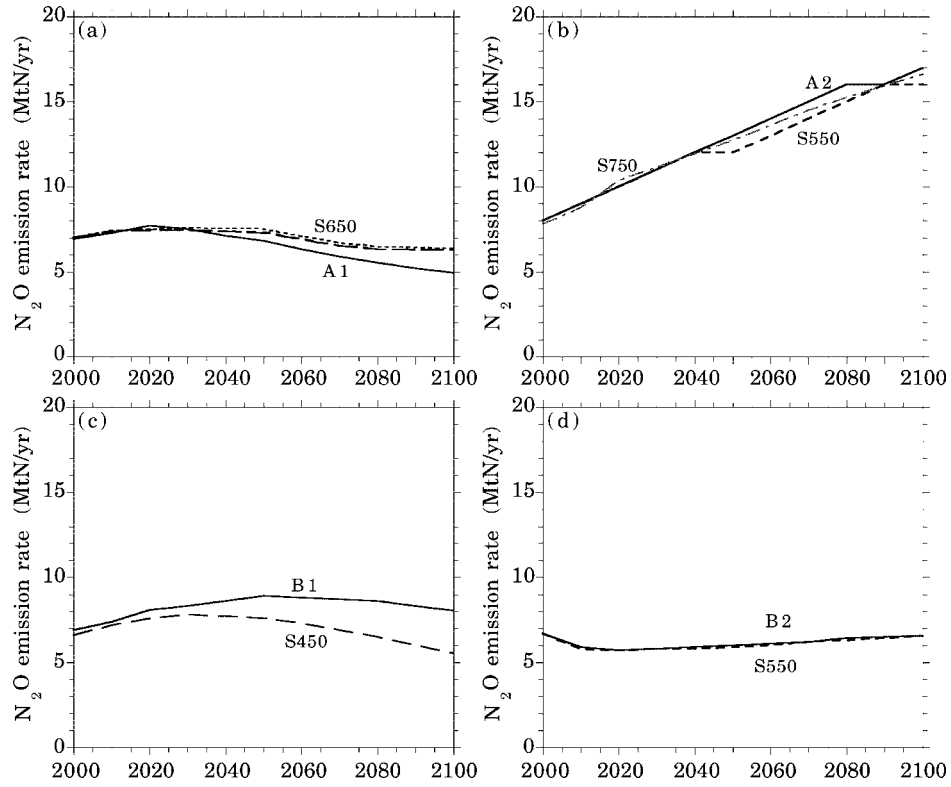

Figure 3. As in figure 1, except for the N_2O emission rates.

such that they have the same emissions individually for 1990 and 2000. We have not performed such a standardization here.

It can be seen from figures 1–4 that not only are the CO_2 emissions for the stabilization scenarios different from their corresponding marker scenarios, so too are the emissions of

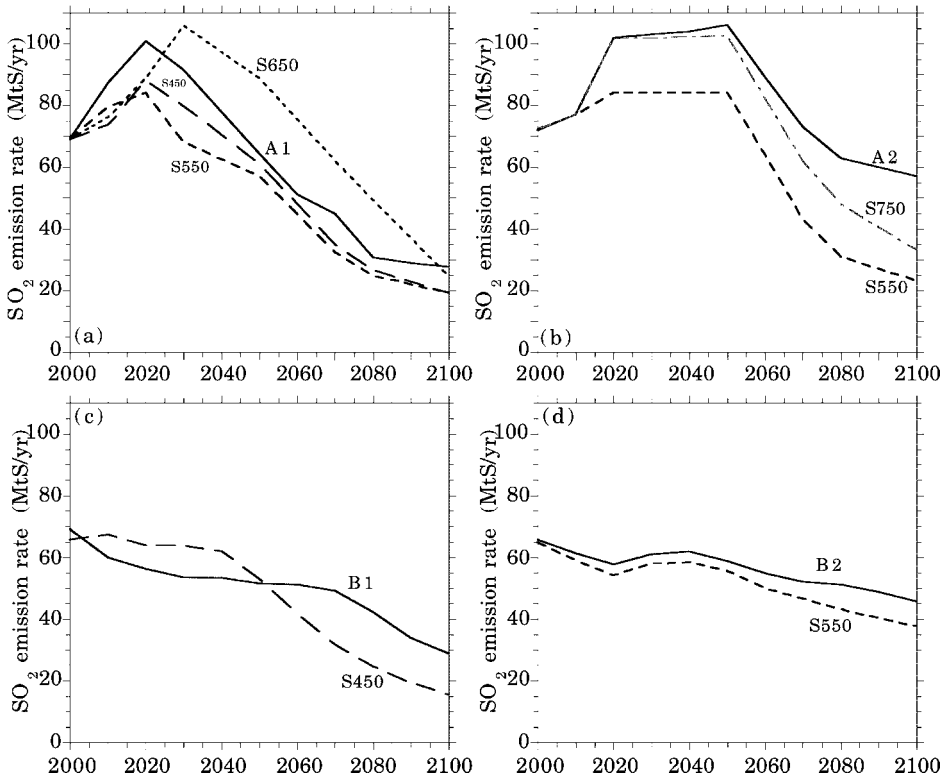

Figure 4. As in figure 1, except for the SO_2 emission rates.

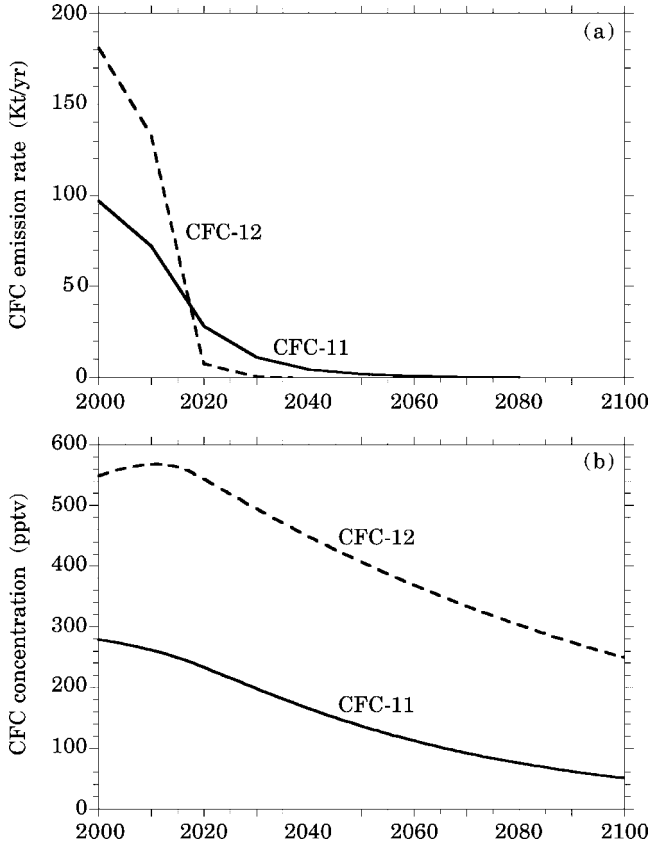

Figure 5. Annual CFC-11 and CFC-12 emission rates (a) and concentrations (b) used for all of the 11 scenarios.

CH_4, N_2O and SO_2. The CFC-11 and CFC-12 emissions (figure 5(a)) are the same for all 11 scenarios, both stabilization and markers.

In general the CO_2 emissions (figure 1) for the stabilization scenarios are lower than for their corresponding markers, but an exception occurs for B1/S450 during part of the first two decades of the 21st century. Similarly, the CH_4 emissions (figure 2) for the stabilization scenarios are lower than for their corresponding markers. The N_2O emissions for the stabilization scenarios (figure 3) are close to those of the corresponding marker scenario for A2 and B2, are less after 2020 for B1, and are greater for A1 after 2030. The SO_2 emissions for the stabilization scenarios (figure 4) are mostly lower than for their corresponding markers, but exceptions occur for A1/S650 after 2025 and B1/S450 before 2050.

3. Concentrations

The resulting concentrations of CO_2 are shown in figure 6 from 2000 to 2300 for the A1-related scenarios, and in figure 7 from 2000 to 2100 for all 11 scenarios. The concentrations of CH_4 and N_2O are shown respectively in figures 8 and 9. The concentrations of CFC-11 and CFC-12 are shown in figure 5.

3.1. CO_2

We have used the carbon-cycle model of the Center for International Climate and Environmental Research – Oslo

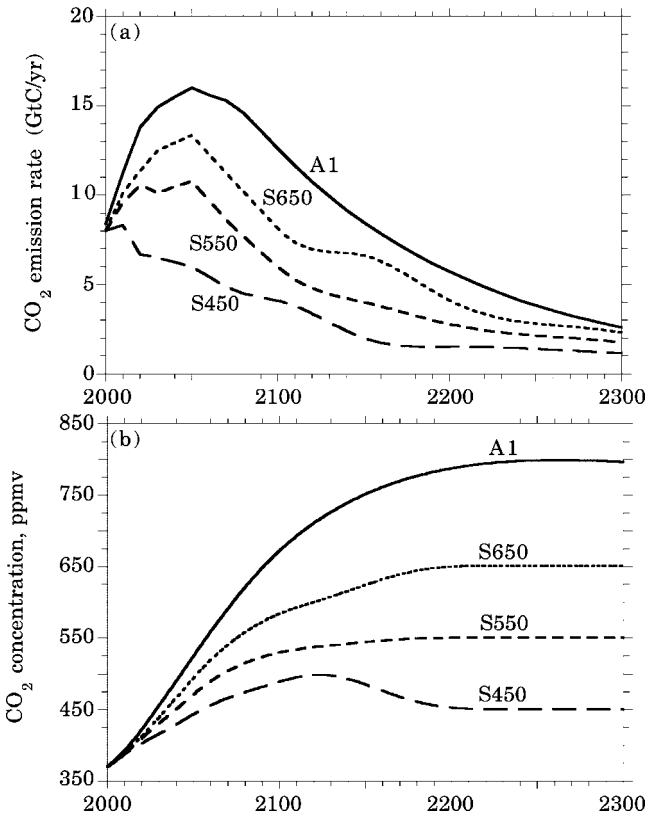

Figure 6. Annual CO_2 emission rate (a) and CO_2 concentration (b) to 2300, respectively for the A1 and B2 SRES marker scenarios and their corresponding Post-SRES stabilization scenarios.

(CICERO) [1], which is based on the work of Joos et al. [12], to calculate the concentrations of CO_2 from its emissions. Our initial calculations with this model yielded stabilized CO_2 concentrations larger than the target values. We traced this to the difference between the CO_2-fertilization (beta) factors in the CICERO and AIM-SSG models – the latter which calculated the emissions – the former using 0.287 and the latter 0.328788. Changing the fertilization factor in the CICERO model to that of the AIM-SSG model decreased the stabilized CO_2 concentration, but the values were still somewhat larger than the targets. Accordingly we replaced the function for the partial pressure of CO_2 in the CICERO code, which for computational economy was evaluated outside that code once-and-for-all for a temperature of 18.2°C, with the temperature-dependent formulation of the AIM-SSG code, which was the same as the unused temperature-dependent formulation in the CICERO code, the difference thus being due to the different precision in the two evaluations. As shown in figure 6 for the A1-related stabilization scenarios, with these changes to the CICERO model, the concentrations do stabilize quite close to their targets early in the 22nd century. Note, however, that for the A1/S450 emissions, the CO_2 concentration overshoots the target in the 21st century and then decreases to the target in the 22nd century. This overshooting does not occur for the higher CO_2 stabilization concentration targets.

Figure 7 shows the CO_2 concentrations for all 11 scenarios during the 21st century. It can be seen that the

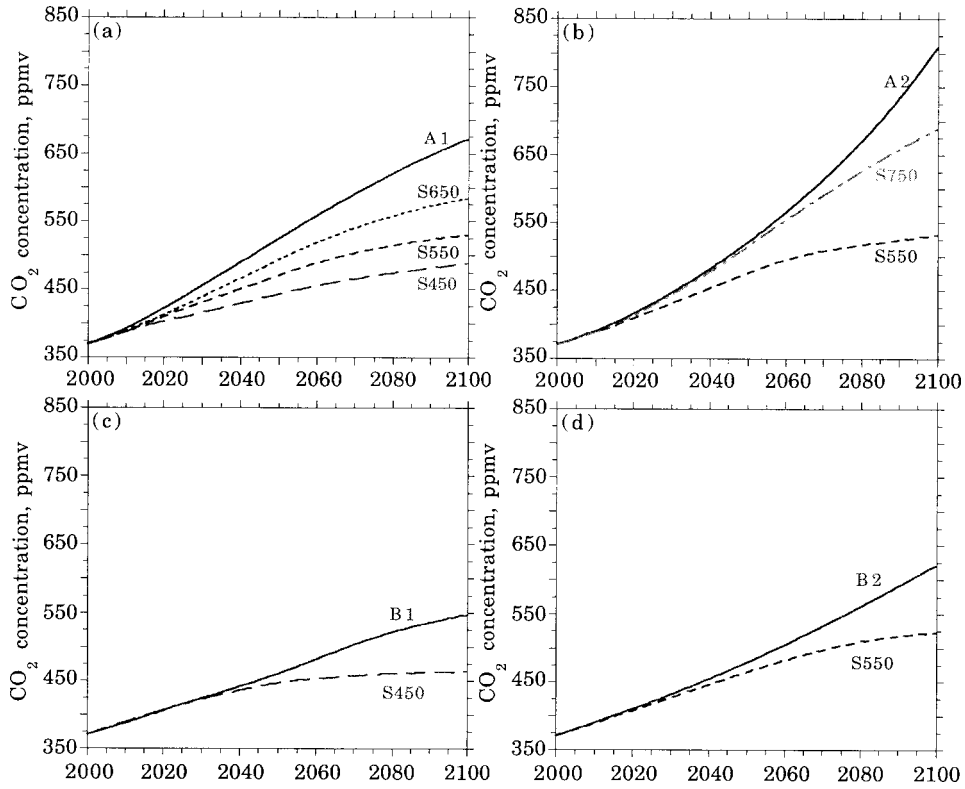

Figure 7. CO_2 concentration for the A1 (a), A2 (b), B1 (c) and B2 (d) SRES marker scenarios and their corresponding Post-SRES stabilization scenarios.

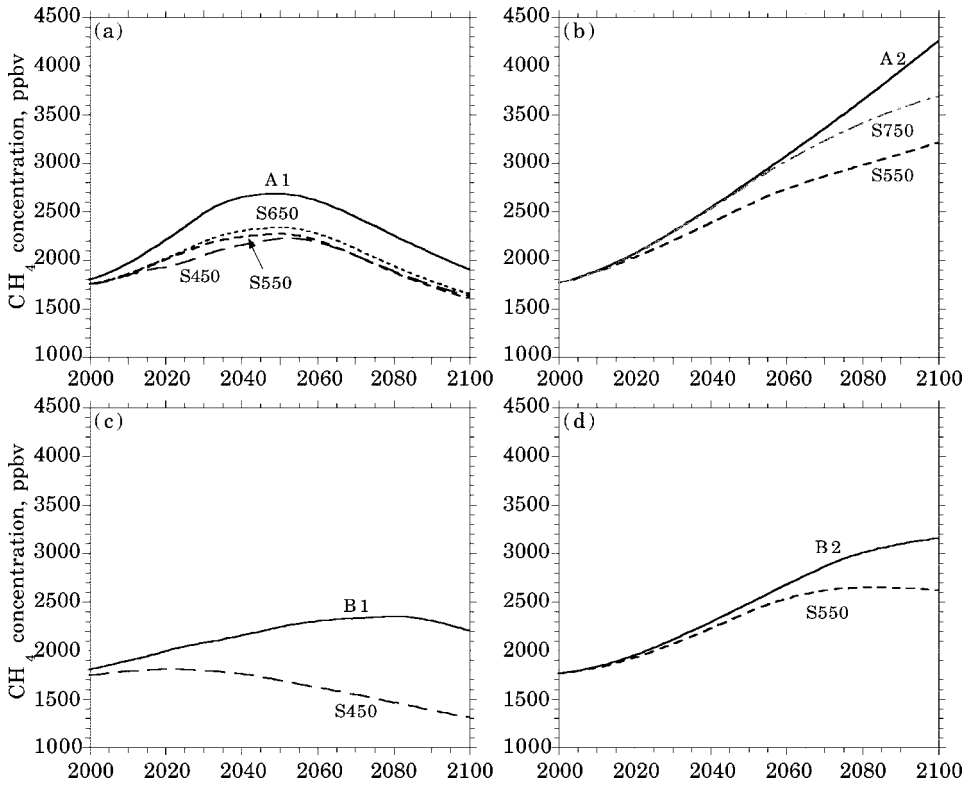

Figure 8. As in figure 7, except for the CH_4 concentration.

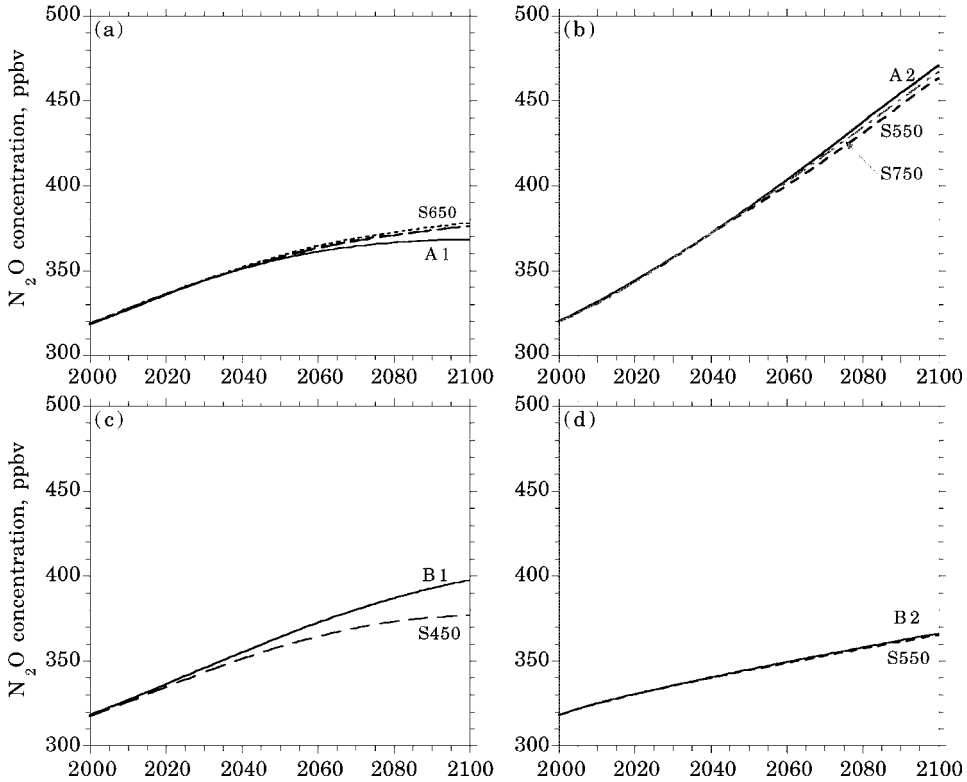

Figure 9. As in figure 7, except for the N_2O concentration.

CO_2 stabilization emission trajectories (figure 1) do result in reduced CO_2 concentrations after some time in the 21st century, earlier for the A1 and A2 stabilization scenarios than for the B1 and B2 stabilization scenarios, and earlier for the lower targets than for the higher targets.

3.2. CH_4, N_2O, CFC-11 and CFC-12

We have used the CICERO emissions-to-concentrations model/code [4] to calculate the concentrations of CH_4, N_2O, CFC-11 and CFC-12 from their emissions. We checked our use of this model by recalculating the CH_4 and N_2O concentrations that were calculated by M. Prather for our climate calculations for the SRES scenarios [37]. We found that the concentrations calculated by the CICERO model with the nonanthropogenic CH_4 and N_2O sources equal to 229 $TgCH_4$/yr and 9 Tg(N)/yr did not agree with the Prather calculations, with the CICERO concentrations rapidly decreasing – for an initial time period for CH_4 and for all times for N_2O – and the Prather concentrations increasing. Accordingly, we adjusted the nonanthropogenic sources to be the difference between the CICERO 1990 total source and the SRES 1990 anthropogenic source. This gave 253 $TgCH_4$/yr and 10.0 TgN_2O-N/yr. With these revised nonanthropogenic emissions the resulting CH_4 and N_2O concentrations using the CICERO code for the SRES scenarios are in excellent agreement with those calculated by Prather.

Figures 8 and 9 present the CH_4 and N_2O concentrations calculated for all 11 emissions scenarios during the 21st century. The lack of standardization for the CH_4 emissions in 2000 is evident in figures 8(a) and 8(c). It can be seen that the CH_4 concentrations for the stabilization scenarios are less than for their corresponding marker scenarios, as are the CH_4 emissions (figure 2), with the largest reductions being for the A2/S550 and B1/S450 scenarios. In contrast, the N_2O concentrations for the stabilization scenarios are quite close to those for their corresponding marker scenarios, as are the N_2O emissions (figure 3), with the exception of the A1 stabilization scenarios, for which the N_2O concentrations exceed those of the A1 scenario, as do the N_2O emissions.

The CFC-11 and CFC-12 concentrations, shown in figure 5(b), decrease with time after the early 21st century as a consequence of the phase-out of their emissions shown in figure 5(a).

4. Changes in global near-surface temperature and sea level

The simulations of the past and future changes in global near-surface temperature and sea level induced by increased GHGs and anthropogenic sulfate aerosol have been performed with our energy-balance-climate/upwelling-diffusion-ocean (EBC/UDO) model.

4.1. The EBC/UDO model

The original, global version of the EBC/UDO model was developed by Schlesinger in 1984, based on the model's original formulation by Hoffert et al. [7], and was used by Schlesinger and colleagues to simulate the global-mean temperature evolution for the different GHG scenarios of the IPCC 1990 report [2], and for greenhouse-policy studies [5,14–16,31,35]. The hemispheric version of the model was developed to study the influence on the climate system of sulfate aerosol (SO_4) created in the atmosphere from the anthropogenic emission of SO_2 [36] and putative solar-irradiance variations [38], and has been used to discover a 65–70 year oscillation in the observed global-mean near-surface temperatures, which was found to occur only over the North Atlantic Ocean and its bordering continental regions [39,40]. A hemispheric version of the model that explicitly calculates the individual temperature changes over land and ocean in each hemisphere [24] has been used to investigate the influence on climate of volcanoes [24] and the influence of global warming on sea level [42]. This hemispheric version of the model, which we use here, was used in conjunction with results from our UIUC 11-layer atmospheric general circulation/mixed-layer-ocean model to calculate the global and geographical climate changes for the SRES marker scenarios [37].

The EBC/UDO model [33] determines the changes in the temperatures of the near-surface air and ocean, the latter as a function of depth from the surface to the ocean floor. The ocean in the model is subdivided vertically into 40 layers, with the uppermost being the 60 m deep mixed layer and the deeper layers each being 100 m thick. Also, the ocean is subdivided horizontally into a polar region where bottom water is formed, and a nonpolar region where there is upwelling. In the nonpolar region, heat is transported upwards toward the surface by the water upwelling there and downwards by physical processes whose effects are treated as an equivalent diffusion. Heat is also removed from the mixed layer in the nonpolar region by a transport to the polar region and downwelling toward the bottom, this heat being ultimately transported upward from the ocean floor in the nonpolar region. The atmosphere in each hemisphere is subdivided into the atmosphere over the ocean and the atmosphere over land, with heat exchange between them. The change in sea level is calculated due to thermal expansion of the ocean and changes in small glaciers and the Antarctic and Greenland ice sheets [33].

We calculate the change in global-mean near-surface temperature and sea level for the SRES marker and Post-SRES scenarios using the EBC/UDO model for three values of temperature sensitivity due to a CO_2 doubling that span the IPCC range – $\Delta T_{2x} = 1.5$, 2.5 and 4.5°C [30].

4.2. Radiative forcing

We have calculated the radiative forcing for CO_2, CH_4, N_2O, CFC-11 and CFC-12 from the equations in table 3 of Myhre et al. [22]. The global radiative forcing by the SO_2 emission is given by [6]

$$F(t) = F^{\mathrm{D}}_{\mathrm{SO_4}}(1990)\left[\frac{E(t)}{E(1990)}\right] + F^{\mathrm{I}}_{\mathrm{SO_4}}(1990)\left[\frac{\ln(1 + E(t)/E_{\mathrm{nat}})}{\ln(1 + E(1990)/E_{\mathrm{nat}})}\right], \quad (1)$$

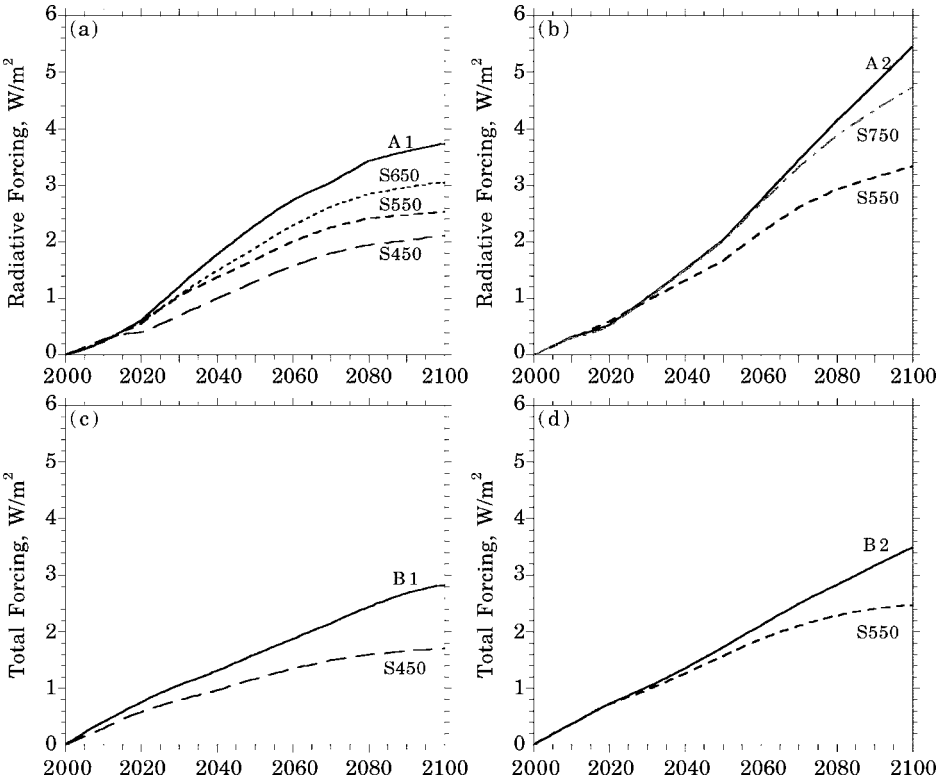

Figure 10. Radiative forcing relative to 2000 for the A1 (a), A2 (b), B1 (c) and B2 (d) SRES marker scenarios and their corresponding Post-SRES stabilization scenarios.

where $E(t)$ is the global anthropogenic emission rate in year t of sulfur in the form of sulfur dioxide, with $E(1990) = 72.6$ TgS/yr; $E_{\rm nat}(t) = 22$ TgS/yr is the global natural SO_2 emission rate; and $F^{\rm D}_{\rm SO_4}(1990) = -0.3\,{\rm W\,m^{-2}}$ and $F^{\rm I}_{\rm SO_4}(1990) = -0.8\,{\rm W\,m^{-2}}$ are the direct (clear-sky) and indirect (cloudy-sky) sulfate radiative forcings in 1990 [6,13]. The calculation was performed from 1860 to 2100, with $E(t)$ given by the historical emissions from 1860 to 1990, and by the scenarios thereafter.

The calculated radiative forcing relative to the year 2000 is presented in figure 10. It is seen that the radiative forcing for the stabilization scenarios is generally smaller than for their corresponding marker scenario, particularly for the A1 and A2 stabilization scenarios, the A2/S550 scenario by about 1 ${\rm W\,m^{-2}}$ in 2100. However, the radiative forcing for the A1/S450 and A2/S550 scenarios slightly exceeds the radiative forcing of their corresponding marker scenario during the early part of the 21st century.

4.3. Changes in global near-surface temperature and sea level

The changes in global near-surface temperature and sea level relative to 2000 are shown respectively in figures 11–13 and 14–16 for $\Delta T_{2x} = 1.5$, 2.5 and 4.5°C – the low, "best-guess" and high estimates of ΔT_{2x} by the IPCC. It can be seen that both the temperature and sea-level responses are qualitatively similar to the corresponding radiative forcing (figure 10), with the changes for the marker scenarios decreasing in the order: A2, A1, B2 and B1. In 2100 the unabated global warming and sea-level rise range from 1.04°C and 22.3 cm for the B1 scenario with $\Delta T_{2x} = 1.5$°C, to 4.07°C and 60.7 cm for the A2 scenario with $\Delta T_{2x} = 4.5$°C. The uncertainty in the temperature response is, on average, 61.6% due to the uncertainty in ΔT_{2x} and 38.4% due to the uncertainty in the scenarios. The uncertainty in the sea-level response is, on average, 68.8% due to the uncertainty in ΔT_{2x} and 31.2% due to the uncertainty in the scenarios. This demonstrates the importance of reducing the uncertainty in ΔT_{2x}.

As an aside, it is of interest to examine the contributions to the total sea-level rise due to its components: ocean thermal expansion, small glaciers, Greenland and Antarctica. These are shown in figure 17 in terms of percentage for the B2 scenario for $\Delta T_{2x} = 1.5$, 2.5 and 4.5°C. Results for the A1, A2 and B1 scenarios are quite close to those for the B2 scenario and are therefore not shown. It can be seen that the contributions by small glaciers and ocean thermal expansion are dominant during the 21st century, each contributing about 45% to the total sea-level rise, with the contribution by glaciers exceeding that by thermal-expansion for a time period at the beginning of the century that decreases with increasing ΔT_{2x}, from about 75 years for $\Delta T_{2x} = 1.5$°C to 30 years for $\Delta T_{2x} = 4.5$°C. The contribution by Antarctica is negative due to the intensification of snow accumulation and cancels about half the positive contribution by Greenland.

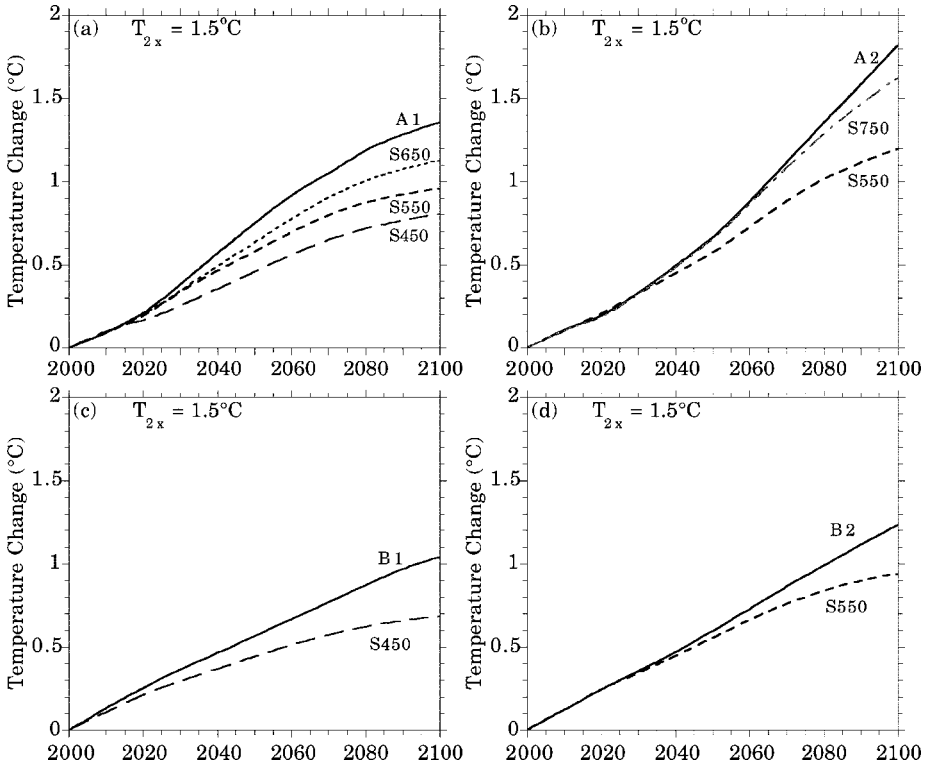

Figure 11. Global-mean near-surface temperature change relative to year 2000 for $\Delta T_{2x} = 1.5°C$ for the A1 (a), A2 (b), B1 (c) and B2 (d) SRES marker scenarios and their corresponding Post-SRES stabilization scenarios.

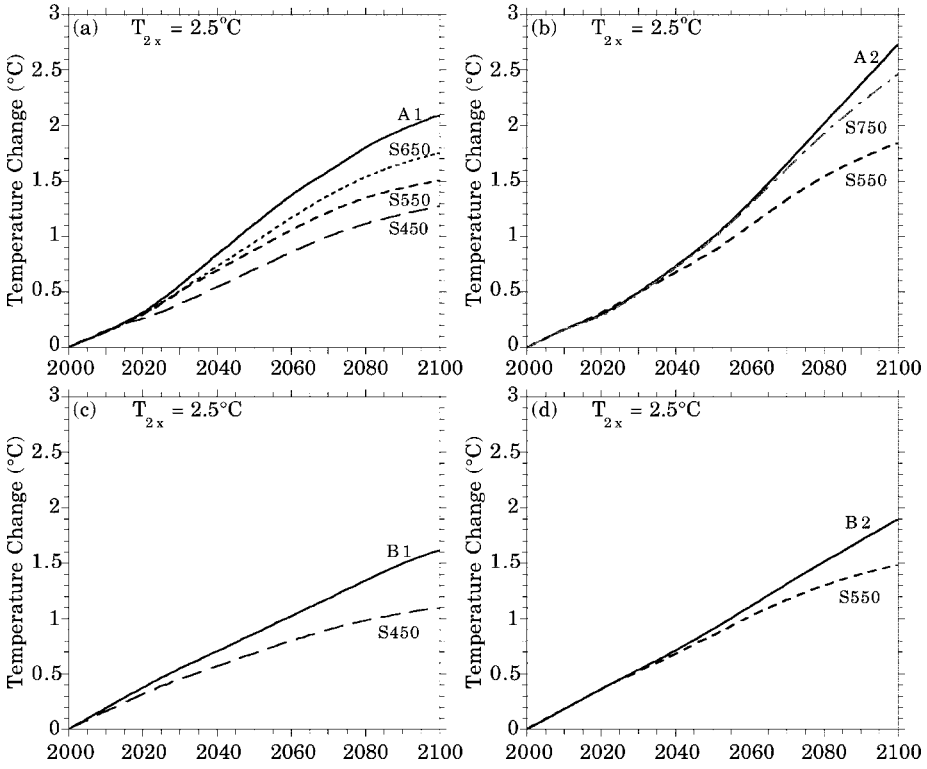

Figure 12. As in figure 11, except for $\Delta T_{2x} = 2.5°C$.

The reductions in global warming and sea-level rise for the stabilization scenarios relative to their corresponding marker scenario (figures 11–16) increases with ΔT_{2x} and is greater the lower the stabilized CO_2 concentration. For the S550 stabilization scenarios, the reduction in global warming and sea-level rise in 2100 range from 0.29°C and 3.31 cm

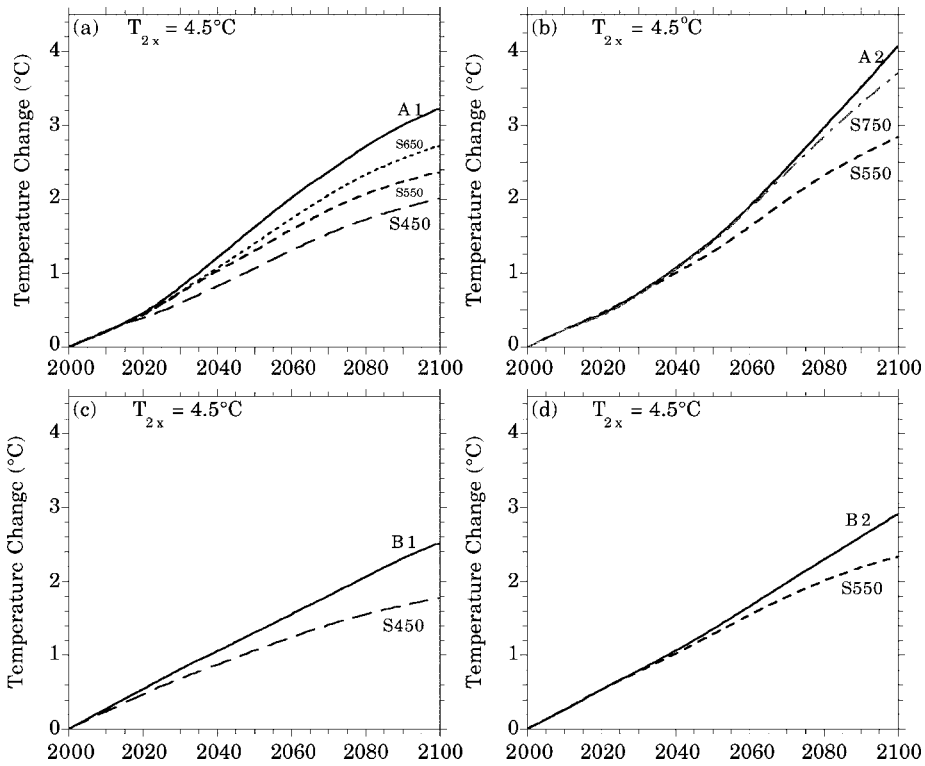

Figure 13. As in figure 11, except for $\Delta T_{2x} = 4.5$°C.

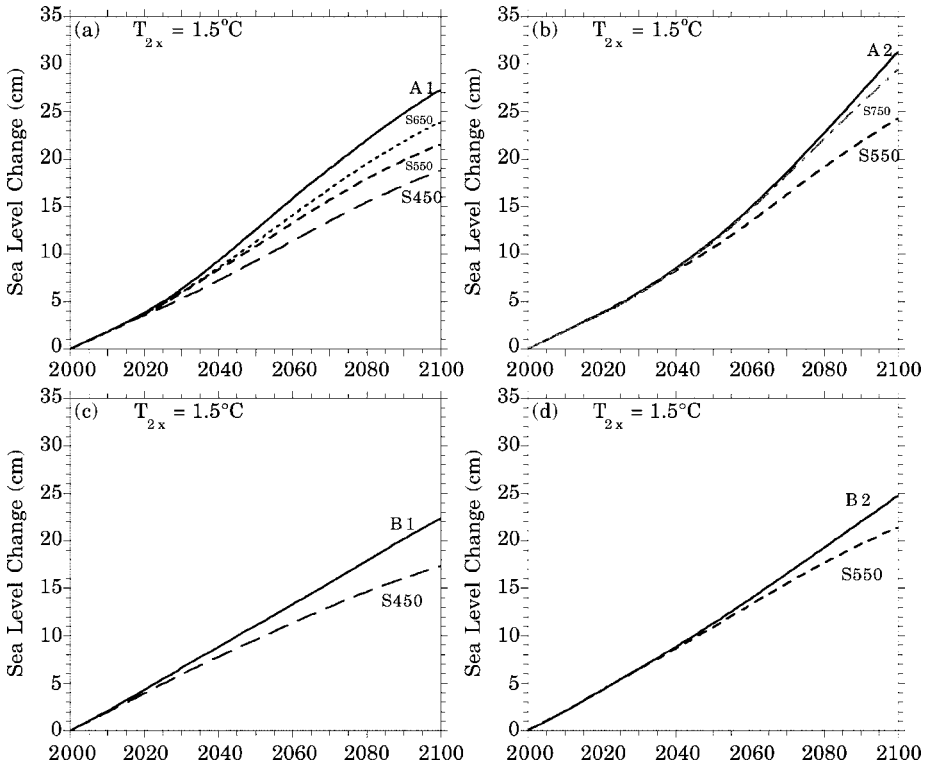

Figure 14. Global-mean sea-level change relative to year 2000 for $\Delta T_{2x} = 1.5$°C for the A1 (a), A2 (b), B1 (c) and B2 (d) SRES marker scenarios and their corresponding Post-SRES stabilization scenarios.

for B2/S550 with $\Delta T_{2x} = 1.5$°C, to 1.22°C and 15.46 cm for A1/S450 with $\Delta T_{2x} = 4.5$°C. The uncertainty in the warming reduction is, on average, 52.7% due to the uncertainty in the scenarios and 47.3% due to the uncertainty in ΔT_{2x}. The uncertainty in the sea-level-rise reduction is, on average, 58.4% due to the uncertainty in the scenarios

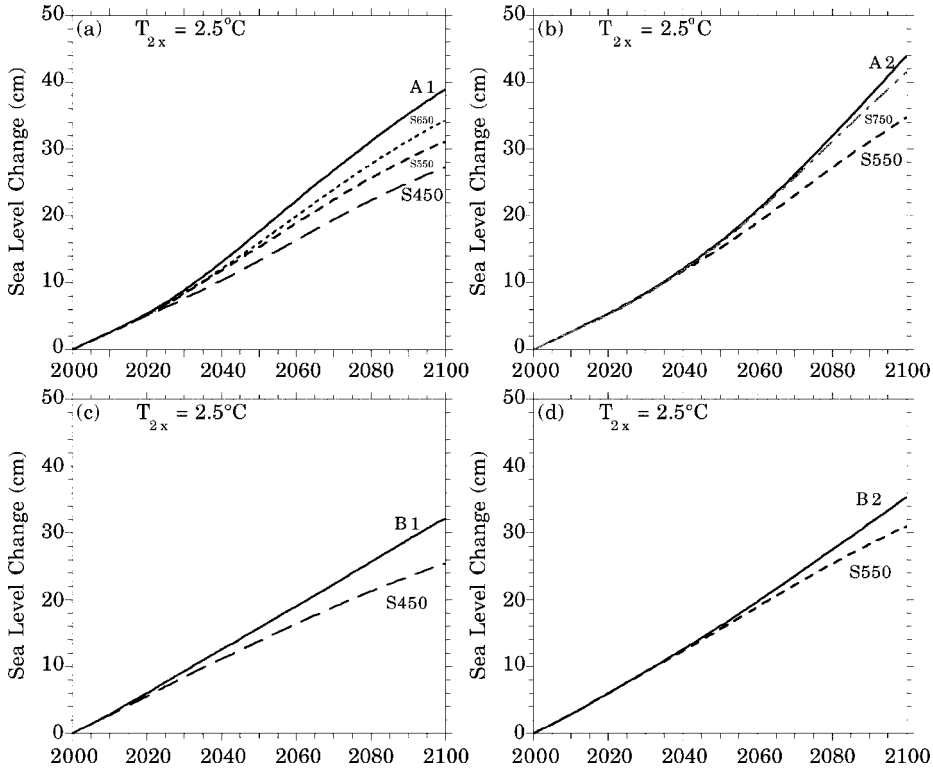

Figure 15. As in figure 14, except for $\Delta T_{2x} = 2.5$°C.

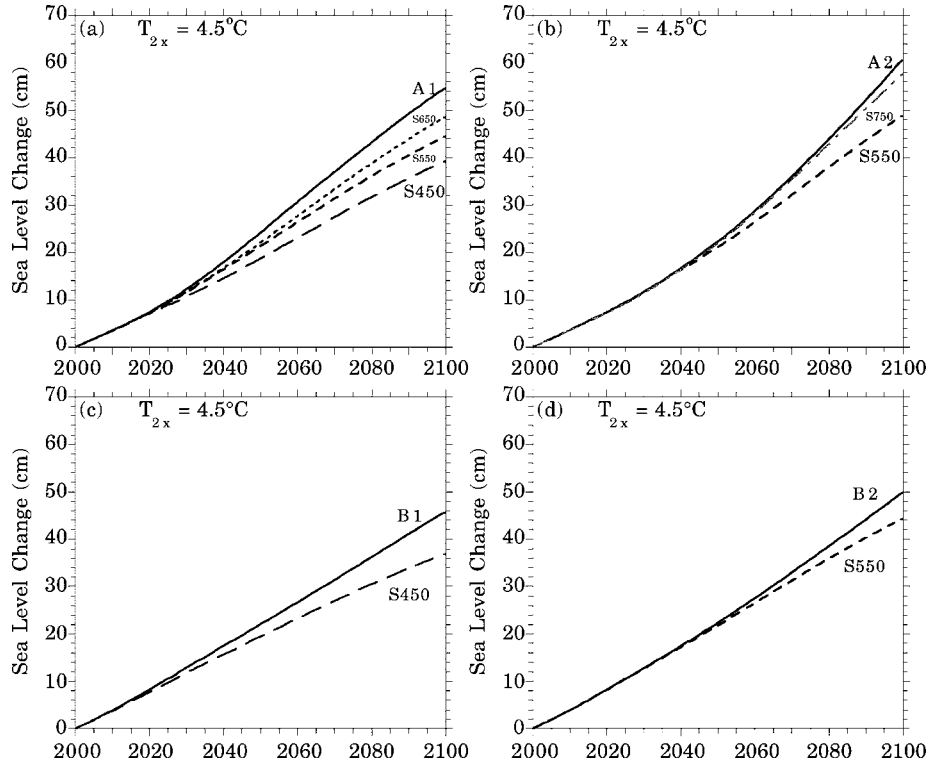

Figure 16. As in figure 14, except for $\Delta T_{2x} = 4.5$°C.

and 41.1% due to the uncertainty in ΔT_{2x}. This illustrates the importance of the scenario uncertainty for the reductions in warming and sea-level rise resulting from stabilizing the CO_2 concentration.

The percent reductions in the global warming and sea-level rise in 2100 are presented in figure 18 for the seven Post-SRES stabilization scenarios and for the three values of ΔT_{2x}. It can be seen that the percent reductions for each sta-

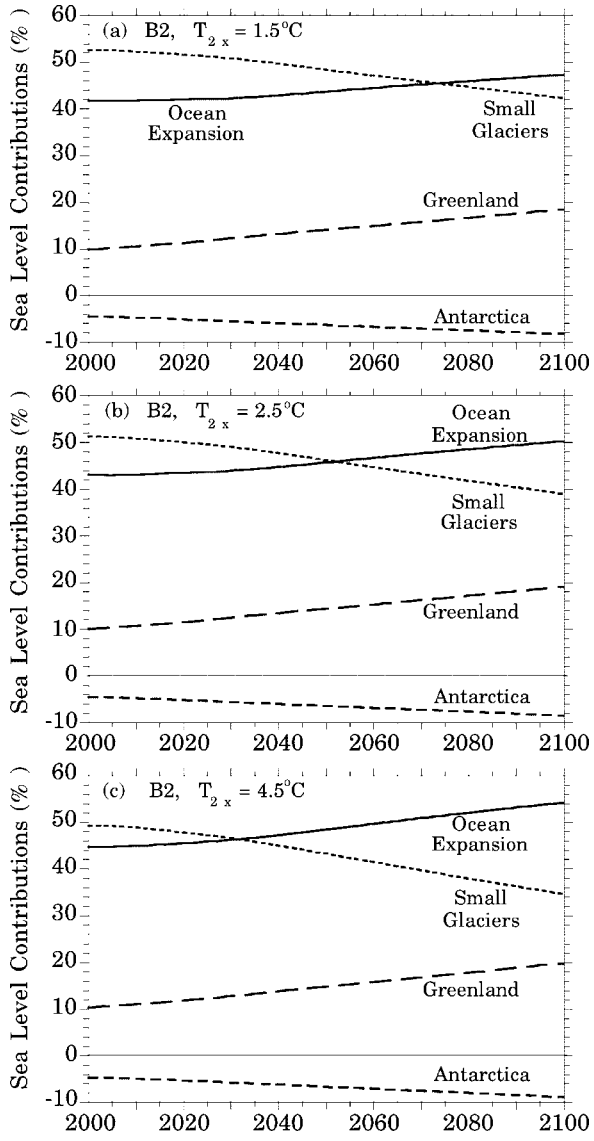

Figure 17. Contributions to total sea-level rise by ocean thermal expansion, small mountain glaciers, Greenland and Antarctica for the A1, A2, B1 and B2 scenario for $\Delta T_{2x} = 1.5°C$ (a), 2.5°C (b) and 4.5°C (c).

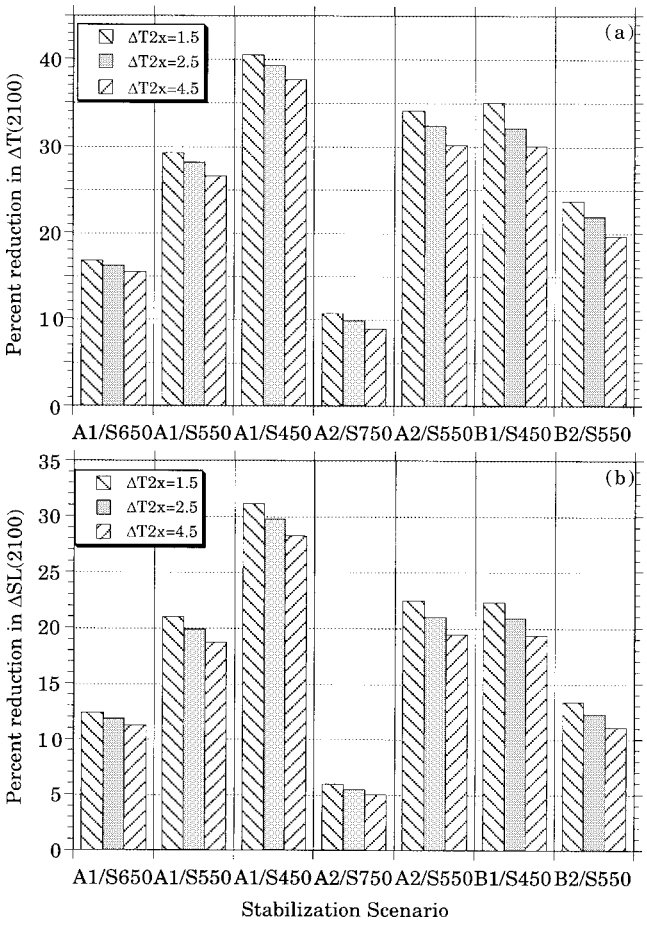

Figure 18. Percentage reduction in the changes relative to year 2000 of global-mean near-surface temperature (ΔT) (a) and sea-level (ΔSL) (b) for the seven Post-SRES stabilization scenarios and three climate sensitivities: $\Delta T_{2x} = 1.5$, 2.5 and 4.5°C.

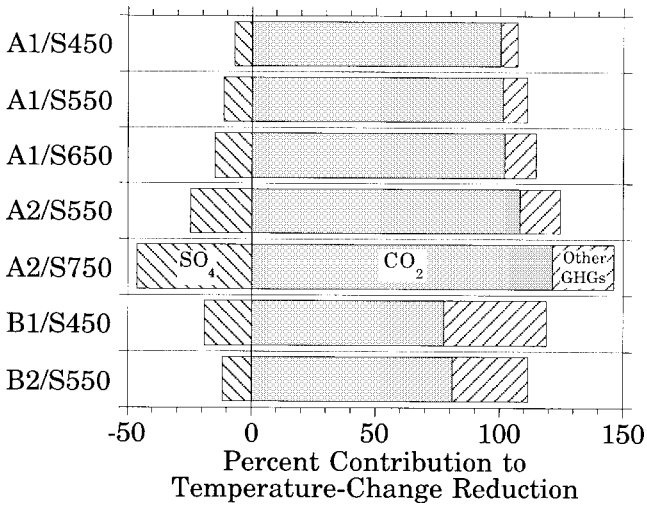

Figure 19. Percent contribution to the reduction in global warming in 2100 by CO_2, the other greenhouse gases (GHGs), and SO_4 for $\Delta T_{2x} = 2.5°C$.

bilization scenario are almost independent of ΔT_{2x}, as was first shown by Schlesinger and Jiang [35]. It can also be seen that the percent reduction in sea-level rise for any stabilization scenario is 4–11% smaller than the corresponding percent reduction in global warming. The percent reductions for the global warming and sea-level rise range respectively from about 10% and 5% for the A2/S750 scenario to about 39% and 30% for the A1/S450 scenario.

It is of interest to examine the contribution of CO_2, the other greenhouses gases in aggregate, and SO_4 to the reduction in global warming. This is shown in figure 19 for $\Delta T_{2x} = 2.5°C$, the results for $\Delta T_{2x} = 1.5°C$ and 4.5°C being virtually identical. It can be seen that the contribution of reduced CO_2 emissions to the reduction in global warming in 2100 ranges from 77% for the B1/S450 scenario to 122% for the A2/S750 scenario. The reason that the CO_2 contribution exceeds the total reduction in global warming is because SO_4 makes a negative contribution that ranges from −7% for the A1/S450 scenario to −46% for the A2/S750 scenario. The SO_4 contribution is negative because the SO_2 emission after 2000 in each stabilization scenario is

smaller than in the corresponding marker scenario (figure 4), and this enhances the warming relative to 2100 already created by the reduction in SO_2 emission in each marker scenario [37]. Put another way, the amelioration of the acid rain problem by the reduction in future emissions of SO_2 exacerbates the global-warming problem. However, the reduction of the other greenhouse gases concomitant with the reduction in CO_2 in the stabilization scenarios aids in the reduction of the global warming in 2100, from 7% in the A1/S450 scenario to 42% in the B1/S450 scenario.

5. Geographical distributions of near-surface temperature change

The geographical distributions of near-surface temperature change are constructed using the superposition method developed by Santer et al. [29]; this method has been used previously by us [19–21,32,34,37,41] and others (e.g., [8, 9]).

The distribution of near-surface temperature change in year t, relative to a reference year – here taken as 2000, as a function of geographical location x is given by

$$\delta T(x,t) = \delta\overline{T}_{\mathrm{GHG}}(t;\Delta T_{2x})\left[\frac{\Delta T_{2x\mathrm{CO}_2}(x)}{\Delta\overline{T}_{2x\mathrm{CO}_2}}\right] + \delta\overline{T}_{\mathrm{SO}_4}(t;\Delta T_{2x})\left[\frac{\Delta T_{10x\mathrm{SO}_4}(x)}{\Delta\overline{T}_{10x\mathrm{SO}_4}}\right], \quad (2)$$

where $\Delta T_{2x\mathrm{CO}_2}(x)$ and $\Delta T_{10x\mathrm{SO}_4}(x)$ are the geographical distributions of the change in equilibrium near-surface temperature, due respectively to a doubling of the CO_2 concentration and a decupling of the SO_4 burden, simulated by our 11-layer atmospheric general circulation/mixed-layer-ocean (AGC/MLO) model [34,37], with $\Delta\overline{T}_{2x\mathrm{CO}_2}$ and $\Delta\overline{T}_{10x\mathrm{SO}_4}$ respectively being their global averages, and $\delta\overline{T}_{\mathrm{GHG}}(t;\Delta T_{2x})$ and $\delta\overline{T}_{\mathrm{SO}_4}(t;\Delta T_{2x})$ are the changes in global-mean near-surface temperature simulated by the EBC/UDO model for year t, relative to the reference year (2000), respectively for the changes in greenhouse-gas concentrations and sulfate-aerosol burden for any SRES or Post-SRES scenario, for any prescribed climate sensitivity, ΔT_{2x}.

The method used in equation (2) is a simplified version of the method we previously used to construct the geographical distributions of near-surface temperature changes for the SRES marker scenarios [37]. In that method the contribution to the temperature change by SO_4 was obtained by a superposition of the normalized near-surface temperature changes from 7 simulations by the AGC/MLO model, one for a tenfold increase in SO_4 burden globally, and 6 for tenfold increases in the SO_4 burden individually for Europe, North Africa, Siberia, Asia, North America and the Southern Hemisphere. We have not used this more elaborate procedure here because we are in the process of extending the control (present climate), $2x\mathrm{CO}_2$ and $10x\mathrm{SO}_4$ simulations made by the 4° latitude by 5° longitude "low-resolution" version of our AGC/MLO model, whose results are used here, by our 4/3° latitude by 4/3° longitude "high-resolution" version of the model. As this high-resolution extension is computationally very expensive, it will not be performed for the foreseeable future for the 6 regional $10x\mathrm{SO}_4$ simulations. Consequently, here we use only the low-resolution simulations that are being extended with the high-resolution model. The method in equation (2) can then be used as is when the high-resolution model simulations are completed.

The constructed geographical distributions of near-surface temperature change are illustrated in figure 20 for the B2/S550 and B2 scenarios in 2100, together with their difference. From the latter it is seen that the near-surface temperature changes of the B2/S550 scenario in 2100 are everywhere smaller than those for the B2 scenario, with values ranging from about 0.3°C in the tropics to 0.5°C over Antarctica and 0.7°C in the Arctic.

6. Conclusion

We have shown that the Post-SRES CO_2-stabilization scenarios reduce the size of anthropogenically induced climate change during the 21st century, particularly during its latter half, by an amount that depends on: (1) the SRES scenario considered, (2) the CO_2 stabilization level, and (3) the climate sensitivity, ΔT_{2x}. Larger reductions in the global near-surface temperature and sea level, and in the geographical distributions of near-surface temperature change are obtained for the gravest SRES scenario, A2; the smallest CO_2 stabilization level considered for that scenario, S550; and the largest climate sensitivity considered, $\Delta T_{2x} = 4.5$°C.

The results of this study can be used in impact analyses and integrated assessments, the latter to determine the benefits of the climate changes foregone by the adoption of a Post-SRES CO_2-stabilization scenario in comparison with its corresponding SRES scenario, and the costs of achieving the CO_2 stabilization through the reduction in CO_2 emissions. To facilitate such impact analyses and integrated assessments, we have put the global results herein presented on our webpage at http://crga.atmos.uiuc.edu/research/post-sres.html. We would be pleased to collaborate in such impact analyses and integrated assessments by calculating the geographical distributions of near-surface temperature and other climatic quantities for the Post-SRES scenarios not presented here, presently using the simulation results from our 4° latitude by 5° longitude atmospheric general circulation/mixed-layer-ocean model, and ultimately the results from our 4/3° latitude by 4/3° longitude model when they become available. We would also be pleased to calculate the time evolutions of global near-surface temperature and sea-level rise for other stabilization scenarios which differ from those presented here either in their target concentration or/and time evolution.

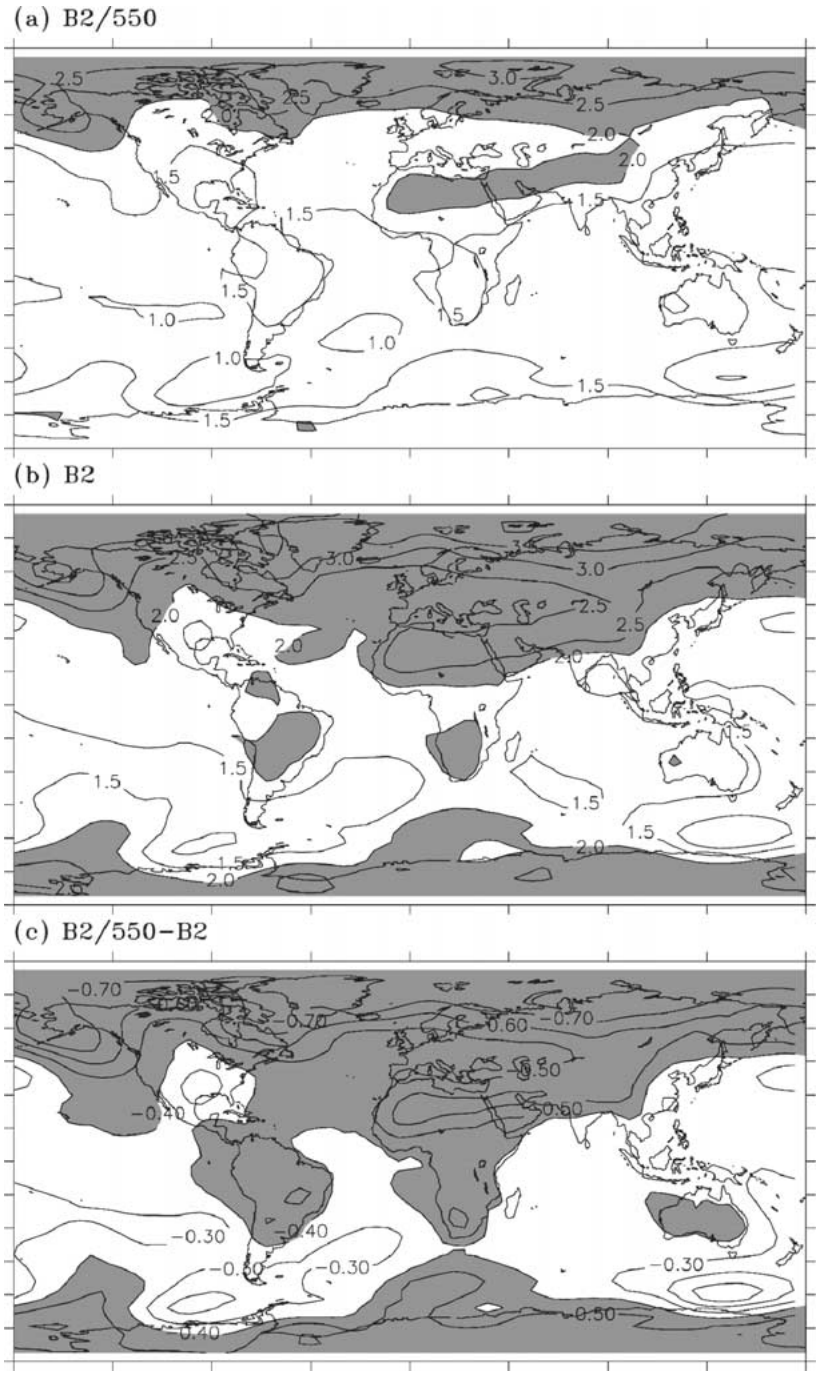

Figure 20. Geographical distributions of the near-surface temperature changes in 2100 relative to 2000 for the B2/S550 (a) and B2 (b) scenarios for $\Delta T_{2x} = 2.5°C$, and the difference between them, B2/S550–B2 (c). In panels (a) and (b) temperature increases in excess of 2°C are shaded. In panel (c) reductions in the warming in excess of 0.3°C are shaded.

Acknowledgements

We thank T. Morita and T. Masui for providing us the A1 scenarios, A. Sankovski the A2 scenarios, B. De Vries the B1 scenarios, and K. Riahi and R.A. Roehrl the B2 scenarios. We thank T.K. Berntsen and J.S. Fuglestvedt for providing us the CICERO code. This study was supported by the U.S. National Science Foundation under Grant ATM 95-22681.

References

[1] K.H. Alfsen and T. Berntsen, An efficient and accurate carbon cycle model for use in simple climate models, CICERO, Oslo, Norway (1999) pp. 14.

[2] F.P. Bretherton, K. Bryan and J.D. Woods, Time-dependent greenhouse-gas-induced climate change, in: *Climatic Change: The IPCC Scientific Assessment*, eds. J.T. Houghton, G.J. Jenkins and J.J. Ephraums (Cambridge University Press, Cambridge, England, 1990) pp. 173–193.

[3] B. de Vries, J. Bollen, L. Bouwman, M. den Elzen, M. Janssen and E. Kreileman, Greenhouse gas emissions in an equity-, environment- and service-oriented world: An IMAGE-based scenario for the next century, Technological Forecasting and Social Change 63(2–3) (2000) 137–174.

[4] J.S. Fuglesvedt and T. Berntsen, A simple model for scenario studies of changes in climate, Version 1.0, CICERO, Oslo, Norway (1999) pp. 59.

[5] J.K. Hammitt, R.J. Lempert and M.E. Schlesinger, A sequential-decision strategy for abating climate change, Nature 357 (1992) 315–318.

[6] L.D.D. Harvey, J. Gregory, M. Hoffert, A. Jain, M. Lal, R. Leemans, S.B.C. Raper, T.M.L. Wigley and J. de Wolde, An introduction to simple climate models used in the IPCC Second Assessment Report, Intergovernmental Panel on Climate Change, Bracknell, UK (1997) pp. 50.

[7] M.I. Hoffert, A.J. Callegari and C.-T. Hsieh, The role of deep sea heat storage in the secular response to climatic forcing, J. Geophys. Res. 85 (1980) 6667–6679.

[8] M. Hulme, T. Jiang and T.M.L. Wigley, SCENGEN, a climate change scenario generator, a user manual, Climatic Research Unit, University of East Anglia, Norwich, UK (1995) pp. 38.

[9] M. Hulme, S.C.B. Raper and T.M.L. Wigley, An integrated framework to address climate change (ESCAPE) and further developments of the global and regional climate modules (MAGICC), Energy Policy 23 (1995) 347–355.

[10] K.T. Jiang, Masui, T. Morita and Y. Matsuoka, Long-term emissions scenarios for China, Environmental Economics and Policy Studies 2(4) (1999) 267–287.

[11] K. Jiang, T. Masui, T. Morita and Y. Matsuoka, Interpretation of the SRES greenhouse gas emissions scenario storylines for Asia-Pacific and the world using the AIM framework, Environmental Economics and Policy Studies (2001).

[12] F. Joos, M. Bruno, R. Fink, U. Siegenthaler, T.F. Stocker, C.L. Quéré and J.L. Sarmiento, An efficient and accurate representation of complex oceanic and biospheric models of anthropogenic carbon uptake, Tellus 48B(3) (1996) 397–417.

[13] A. Kattenberg, F. Giorgi, H. Grassl, G.A. Meehl, J.B.F. Mitchell, R.J. Stouffer, T. Tokioka, A.J. Weaver and T.M.L. Wigley, Climate models – Projections of future climate, in: *Climate Change 1995: The Science of Climate Change*, eds. J.T. Houghton, L.G. Meira Filho, B.A. Callander, N. Harris, A. Kattenberg and K. Maskell (Cambridge University Press, Cambridge, UK, 1996) pp. 285–358.

[14] R.J. Lempert, M.E. Schlesinger and S.C. Bankes, When we don't know the costs or the benefits: Adaptive strategies for abating climate change, Climatic Change 33 (1996) 235–274.

[15] R.J. Lempert, M.E. Schlesinger, S.C. Bankes and N.G. Andronova, The impacts of climate variability on near-term policy choices and the value of information, Climatic Change 45(1) (2000) 129–161.

[16] R.J. Lempert, M.E. Schlesinger and J.K. Hammitt, The impact of potential abrupt climate changes on near-term policy choices, Climatic Change 26 (1994) 351–376.

[17] Y. Matsuoka, Extrapolation of carbon dioxide emission scenarios to meet long-term atmospheric stabilization targets, Environmental Economics and Policy Studies 3(2) (2000) 255–265.

[18] Y. Matsuoka, Development of a stabilization scenario generator for long-term climatic assessment, Environmental Economics and Policy Studies (2001) (in press).

[19] R. Mendelsohn, W. Morrison, M.E. Schlesinger and N.G. Andronova, Country-specific market impacts of climate change, Climatic Change 45(3–4) (2000) 553–569.

[20] R. Mendelsohn, M. Schlesinger and L. Williams, The climate impacts of sulfate aerosols, Integrated Assessment (2001) 111–122.

[21] R. Mendelsohn, M.E. Schlesinger and L. Williams, Comparing impacts across climate models, Integrated Assessment 1 (2000) 37–48.

[22] G. Myhre, E.J. Highwood, K.P. Shine and F. Stordal, New estimates of radiative forcing due to well mixed greenhouse gases, Geophys. Res. Lett. 25(14) (1998) 2715–2718.

[23] N. Nakicenovic and R. Swart, eds., *IPCC Special Report on Emissions Scenarios* (Cambridge University Press, Cambridge, 2000) pp. 612.

[24] N. Ramankutty, An empirical estimate of climate sensitivity, M.S. Thesis, University of Illinois at Urbana-Champaign, Urbana, IL (1994) pp. 174.

[25] K. Riahi and R.A. Roehrl, Greenhouse gas emissions in a dynamics as usual scenario of economic and energy development, Technological Forecasting and Social Change 63(2–3) (2000).

[26] K. Riahi and R.A. Roehrl, Robust energy technology strategies for the 21st century – Carbon dioxide mitigation and sustainable development, Environmental Economics and Policy Studies (2000) 89–125.

[27] A. Sankovski, W. Barbour and W. Pepper, Quantification of the IS99 emission scenario storylines using the Atmospheric Stabilization Framework (ASF), Technological Forecasting and Social Change 63(2–3) (2000) 263–287.

[28] A. Sankovski, W. Barbour and W. Pepper, Climate change mitigation in regionalized world, Environmental Economics and Policy Studies (2001) (in press).

[29] B.D. Santer, T.M.L. Wigley, M.E. Schlesinger and J.F.B. Mitchell, Developing climate scenarios from equilibrium GCM results, Max-Planck-Institut für Meteorologie, Hamburg, Germany (1990) pp. 29.

[30] D. Schimel, D. Alves, I. Enting, M. Heimann, F. Joos, D. Raynaud, T. Wigley, M. Prather, R. Serwent, D. Ehhalt, P. Fraser, E. Sanhueza, X. Zhou, P. Jonas, R. Charlson, H. Rodhe, S. Sadasivan, K.P. Shine, Y. Fouquart, V. Ramaswamy, S. Solomon, J. Srinivasan, D. Albritton, R. Derwent, I. Isaksen, M. Lal and D. Wuebbles, Radiative forcing of climate change, in: *Climate Change 1995: The Science of Climate Change*, eds. J.T. Houghton, L.G. Meira Filho, B.A. Callander, N. Harris, A. Kattenberg and K. Maskell (Cambridge University Press, Cambridge, 1996) pp. 65–132.

[31] M.E. Schlesinger, Greenhouse policy, National Geographic Research & Exploration 9(2) (1993) 159–172.

[32] M.E. Schlesinger and N. Andronova, Regional climate-change scenarios based on $2xCO_2$ and $4xCO_2$ equilibrium climate-changes simulated by the UIUC atmospheric general circulation/mixed-layer ocean model, Urbana, IL (1994) pp. 14.

[33] M.E. Schlesinger, N.G. Andronova, B. Entwistle, A. Ghanem, N. Ramankutty, W. Wang and F. Yang, Modeling and simulation of climate and climate change, in: *Past and Present Variability of the Solar-Terrestrial System: Measurement, Data Analysis and Theoretical Models. Proceedings of the International School of Physics "Enrico Fermi" CXXXIII*, eds. G. Cini Castagnoli and A. Provenzale (IOS Press, Amsterdam, 1997) pp. 389–429.

[34] M.E. Schlesinger, N. Andronova, A. Ghanem, S. Malyshev, T. Reichler, E. Rozanov, W. Wang and F. Yang, Geographical scenarios of greenhouse-gas and anthropogenic-sulfate-aerosol induced climate changes, Climate Research Group, Department of Atmospheric Sciences, University of Illinois at Urbana-Champaign, Urbana, IL (1997) pp. 86.

[35] M.E. Schlesinger and X. Jiang, Revised projection of future greenhouse warming, Nature 350 (1991) 219–221.

[36] M.E. Schlesinger X. Jiang and R.J. Charlson, Implication of anthropogenic atmospheric sulphate for the sensitivity of the climate system, in: *Climate Change and Energy Policy: Proceedings of the International Conference on Global Climate Change: Its Mitigation Through Improved Production and Use of Energy*, eds. L. Rosen and R. Glasser (American Institute of Physics, New York, 1992) pp. 75–108.

[37] M.E. Schlesinger, S. Malyshev, E.V. Rozanov, F. Yang, N.G. Andronova, B. de Vries, A. Grübler, K. Jiang, T. Masui, T. Morita, J. Penner, W. Pepper, A. Sankovski and Y. Zhang, Geographical distributions of temperature change for scenarios of greenhouse gas and sulfur dioxide emissions, Technological Forecasting and Social Change 65 (2000) 167–193.

[38] M.E. Schlesinger and N. Ramankutty, Implications for global warming of intercycle solar-irradiance variations, Nature 360 (1992) 330–333.

[39] M.E. Schlesinger and N. Ramankutty, An oscillation in the global climate system of period 65–70 years, Nature 367 (1994) 723–726.

[40] M.E. Schlesinger and N. Ramankutty, Is the recently reported 65–70 year surface-temperature oscillation the result of climatic noise?, J. Geophys. Res. 100 (1995) 13 767–13 774.

[41] M.E. Schlesinger and L.J. Williams, COSMIC – Country Specific Model for Intertemporal Climate, Electric Power Research Institute, Palo Alto (1997).

[42] G.W. Yohe and M.E. Schlesinger, Sea level change: The expected economic cost of protection or abandonment in the United States, Climatic Change 38 (1998) 447–472.